A Class of Broadband Three-Port TEM-Mode Hybrids

SEYMOUR B. COHN, FELLOW, IEEE

Abstract—The three-port hybrid considered in this paper is useful both as a power divider and power combiner. In the divider application, power entering the input port is split equally and with zero phase difference between the output ports. All ports are well matched and the output ports are highly isolated. The generalized form of the hybrid circuit is a T junction followed by a multiplicity of cascaded pairs of TEM line lengths and interconnecting resistors. Due to symmetry, the resistors are decoupled from the input port, but they serve an essential function in providing output-port match and isolation. Each pair of lines and its associated resistor are referred to as a section. The one-section hybrid has been known and widely used. Its usable bandwidth is $f_2/f_1 = 1.44:1$ for VSWR <1.22 and isolation >20 dB. This paper shows that additional sections can provide a large increase in bandwidth. Some of the examples treated are as follows: two sections, $f_2/f_1 = 2$, VSWR <1.11, isolation >27 dB; four sections, $f_2/f_1 = 4$, VSWR <1.10, isolation >26 dB; and seven sections, $f_2/f_1 = 10$, VSWR <1.21, isolation >19 dB. Exact design formulas are given for two-section hybrids, and approximate design formulas for three or more sections.

I. INTRODUCTION

THE THREE-PORT hybrid considered in this paper is equivalent to a conventional four-port T hybrid whose series port is terminated internally by a reflectionless load. Power entering the shunt port emerges with equal amplitude and phase at the other two ports. Each of the three ports has nearly unity VSWR, while isolation of the output ports is high. In addition to its application as a power divider, reciprocity allows this type of hybrid junction to function as a lossless power combiner of two equal in-phase signals.

Several papers have been published on three-port hybrids. The earliest known to this author is by Wilkinson, treating n output-port ($n \geq 2$) power division.[1] With $n = 2$ his circuit reduces to that shown in Fig. 1. The theoretical VSWR's and isolation are plotted in this figure. For bandwidths up to about 1.4:1 the performance is quite good, but at the edges of a 2:1 band the isolation is only 14.7 dB and the input-port VSWR is 1.42. (In all cases of VSWR and isolation data, the ports not connected are assumed terminated by Z_0 loads.) Shortly after Wilkinson's paper appeared, Dent published the same three-port circuit and included confirming experimental data.[2]

Parad and Moynihan published a more complex version of Fig. 1, allowing unequal as well as equal power division.[3]

The author was with the Rantec Division, Emerson Electric Co., Calabasas, Calif. He is now a consultant for Rantec and other, at 5021 Palomar Drive, Tarzana, Calif., 91356
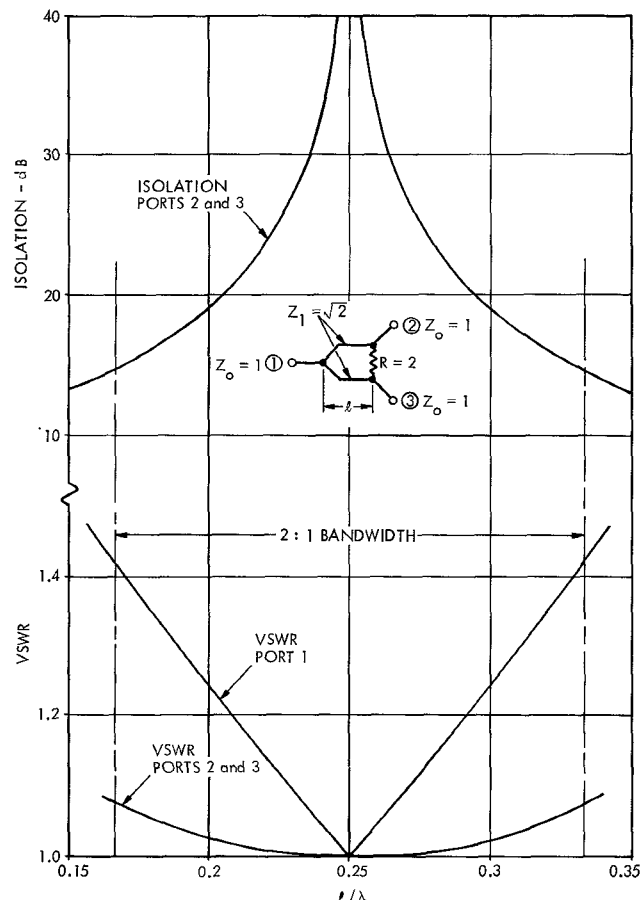
Fig. 1.   Basic three-port hybrid and its VSWR and isolation response.

Their best design example covers a 1.57:1 band with maximum VSWR equal to 1.20 and minimum isolation about 20 dB. David has shown a modification of Fig. 1 in which open-circuited coaxial lines are inserted in series with the output ports.[4] This yields enhanced bandwidth with VSWR's less than 1.4 and isolation greater than 19 dB in a 2:1 band.

These previously published designs utilize a three-port circuit of varying complexity plus a resistor. (Wilkinson generalizes this to an n-way junction with a resistor between each adjacent pair of output ports.) The broadband three-port hybrids presented in this paper differ in that they contain a multiplicity of cascaded pairs of line lengths and interconnecting resistors. Compared to the earlier designs, an enormous improvement in VSWR and isolation is obtained over a given bandwidth, even when only two pairs of lines and two resistors are used. As the number of line

sections and resistors is increased, the bandwidth capability improves without limit.

II. GENERALIZED CIRCUIT AND ANALYSIS OF PERFORMANCE

Fig. 2(a) shows the general circuit of the class of three-port hybrids treated in this paper. This is an "N-section" circuit, containing N pairs of equal-length transmission lines and N bridging resistors distributed from port 1 to ports 2 and 3. Fig. 2(b) shows a specialization of this circuit in which the quantity of resistors is reduced by letting one or more be zero ohms and one or more be infinite ohms. As additional generalizations, the multisection technique may be used to increase the bandwidth of Wilkinson's n-way power divider[1] and also Parad and Moynihan's unequal power-split power divider.[3]

The symmetrical power-divider circuit in Fig. 2(a) is most easily analyzed by the method of even- and odd-mode excitations of ports 2 and 3 with a Z_0 load connected to port 1. This method has been discussed by Reed and Wheeler[5] for the case of four-port symmetrical structures. Their results may be applied with only slight adaptation to the three-port case of Fig. 2(a).

With even-mode excitation, waves of equal amplitude and zero phase difference are incident on ports 2 and 3. The voltage difference is then zero between all pairs of corresponding junction points along the upper and lower transmission paths in Fig. 2(a), and no power is dissipated in the resistors. The power output at port 1 is the total power incident at ports 2 and 3 minus the total reflected power. Because there is no transverse current flow, the circuit in Fig. 2(a) can be bisected symmetrically by a longitudinal nonconducting wall. The resulting circuit is shown in Fig. 3(a). Note that the left-hand load is replaced by 2 Z_0 as a result of the bisection.

With odd-mode excitation at ports 2 and 3, waves of equal amplitude and 180° phase difference travel along the two transmission paths. The resistors then have substantial voltages impressed across them. Due to symmetry, the midpoints of the resistors and the junction of the lines at port 1 are at ground potential. Therefore the bisected circuit is as shown in Fig. 3(b).

Fig. 3(c) and (d) is equivalent to Fig. 3(a) and (b) except that it has been reversed so that the incident waves arrive from the left. Because an admittance representation is more convenient, the following substitutions have been made

$$Y_1 = 1/Z_1, \qquad Y_2 = 1/Z_2, \cdots, \qquad Y_N = 1/Z_N$$

$$G_1 = 1/R_1, \qquad G_2 = 1/R_2, \cdots, \qquad G_N = 1/R_N$$

$$Y_0 = 1/Z_0 = 1, \qquad G_L = 1/2Z_0 = 0.5. \tag{1}$$

Each Y_k value is assumed unaffected by a change from even to odd excitation. This requires coupling between adjacent conductors to be small. If the weak coupling condition is violated, then Y_k (odd) $>$ Y_k (even), resulting in some degradation of performance and greater design difficulty.

Let ρ_e and ρ_0 be the voltage reflection coefficients of the circuits in Fig. 3(c) and (d). Also, let ρ_1, ρ_2, and ρ_3 be the voltage reflection coefficients at ports 1, 2, and 3 of the
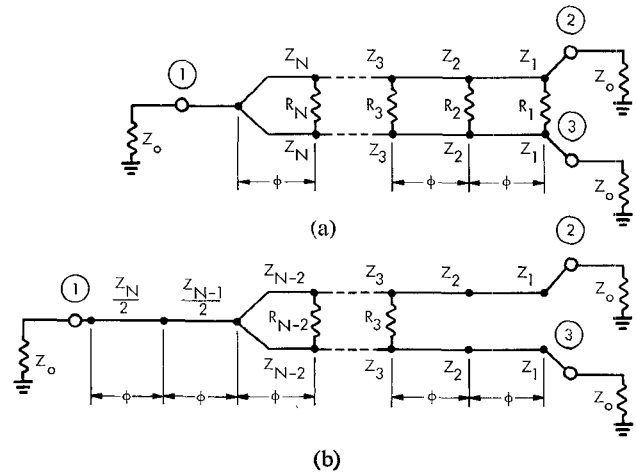

Fig. 2. General circuit of the multiple-section three-port hybrid and an example of a special case. (a) General circuit. (b) Special case of $R_1 = R_2 = \infty$ and $R_{N-1} = R_N = 0$.
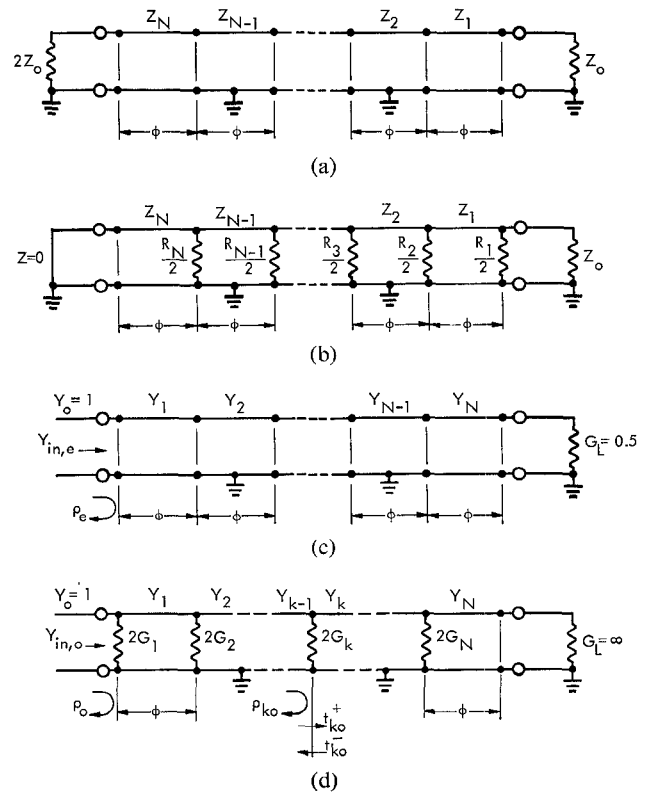

Fig. 3. Bisection circuits for even and odd modes. (a) Bisection for even mode. (b) Bisection for odd mode. (c) Admittance circuit, even mode. (d) Admittance circuit, odd mode.

complete power divider of Fig. 2(a), and t_{12}, t_{13}, and t_{23} be the voltage transmission coefficients between these ports. Then adapting Reed and Wheeler's results to the symmetrical three-port case

$$|\rho_1| = |\rho_e| \tag{2}$$

$$t_{12} = t_{13}; \qquad |t_{12}| = |t_{13}| = \sqrt{\tfrac{1}{2}(1 - \rho_e{}^2)} \tag{3}$$

$$\rho_2 = \rho_3 = \tfrac{1}{2}(\rho_e + \rho_o) \tag{4}$$

$$t_{23} = \tfrac{1}{2}(\rho_e - \rho_o). \tag{5}$$

Thus the reflection coefficients ρ_e and ρ_o of the bisected circuits in Fig. 3(c) and (d) are sufficient data for the computation of all reflection and transmission coefficients of the general three-port symmetrical circuit of Fig. 2(a).

III. SYNTHESIS FOR OPTIMUM PERFORMANCE

The power-divider circuit is composed of a finite number of resistors and equal line lengths. Therefore, the input impedances and various reflection and transmission coefficients can be expressed as quotients of polynomials in s of finite degree, where[6]

$$s = -j \cot \phi. \tag{6}$$

Synthesis for optimum performance in a given bandwidth is thus reduced to an algebraic problem involving "positive-real" rational input-impedance functions of the complex variable s. By optimum performance is meant equal-ripple (Chebyshev) behavior of ρ_1, ρ_2, ρ_3, and t_{12} in a specified bandwidth, the number of ripples being the maximum possible for the number of circuit sections N.

The synthesis problem is simplified by seeing that the even-mode circuit of Fig. 3(c) is a stepped transformer between terminal conductances 1 and 0.5. Thus $|\rho_1| = |\rho_e|$ will have optimum equal-ripple behavior if the characteristic admittances $Y_1, Y_2, \cdots, Y_N$ are designed to yield optimum stepped-transformer response. Formulas and tables for determining Y_1 to Y_N are available and need not be reproduced here.[7],[8] With the characteristic admittances determined, the remainder of the synthesis problem is to compute the conductances $G_1, G_2, \cdots, G_N$ such that ρ_2, ρ_3, and t_{23} are optimum. It is much easier, however, to compute G_1 to G_N such that ρ_o is optimized. A number of computed cases show that when ρ_e and ρ_o are optimum, ρ_2 and t_{23} are very close to optimum.

An almost exact synthesis is quite simple for $N=2$, but is increasingly difficult for $N \geq 3$. The $N=2$ case is treated in Section IV. For $N \geq 3$ a set of approximate design formulas has been deduced heuristically and is given in Section V.

IV. DESIGN FORMULAS, $N=2$

Fig. 4 shows the general shape of $|\rho_o|$ vs. ϕ. This function is symmetrical about $\phi=90°$, and has a ripple maximum at $90°$ and zero points at ϕ_3 and $\phi_4=180°-\phi_3$. The equal-ripple band edges are ϕ_1 and $\phi_2=180°-\phi_1$. The $|\rho_e|$ function is similar in shape to $|\rho_o|$, also having one maximum and two zeros. When $N=2$, the input admittance and reflection coefficient in Fig. 3(d) are determined as follows by means of elementary transmission-line theory
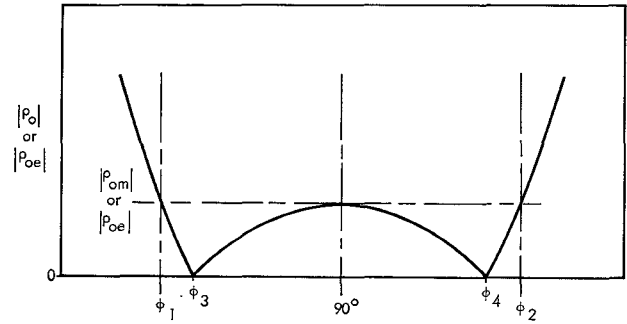

Fig. 4. General equal-ripple shape of $|\rho_o|$ and $|\rho_e|$ functions, two-section case.

are imaginary, the following relations hold at ϕ_3

$$2G_2(1 - 2G_1) - Y_1{}^2 - Y_1 Y_2 s^2 = 0 \tag{9}$$

$$(Y_1 + Y_2)(1 - 2G_1) - 2G_2 Y_1 = 0. \tag{10}$$

Equations (1), (6), (9) and (10) yield

$$R_2 = \frac{2Z_1 Z_2}{\sqrt{(Z_1 + Z_2)(Z_2 - Z_1 \cot^2 \phi_3)}} \tag{11}$$

$$R_1 = \frac{2R_2(Z_1 + Z_2)}{R_2(Z_1 + Z_2) - 2Z_2}. \tag{12}$$

A formula relating ϕ_3 to ϕ_1 is obtained from $|\rho_0| \propto T_2(x) = 2x^2 - 1$, where $x=(90°-\phi)/(90°-\phi_1)$. The function $T_2(x)$ is the Chebyshev polynomial of second degree. The result is

$$\phi_3 = 90° - \frac{1}{\sqrt{2}} (90° - \phi_1)$$

$$= 90° \left[1 - \frac{1}{\sqrt{2}} \left(\frac{f_2/f_1 - 1}{f_2/f_1 + 1} \right) \right]. \tag{13}$$

A formula for ϕ_3 based on $x = \cos \phi / \cos \phi_1$ instead of $x=(90°-\phi)/(90°-\phi_1)$ might be thought more accurate; however, detailed computation shows (13) to give better results.

The maximum VSWR's at the three ports and minimum isolation may be computed from (2), (4) and (5), letting $\phi=90°$. However, the approximate formulas (22), (23) and (24) in Section VI offer good accuracy and simplicity.

Equations (11), (12) and (13) are the design formulas for the two-section case. First, Z_1 and Z_2 are computed as stepped-transformer sections matching the terminating con-

$$Y_{in,o} = 2G_1 + Y_1 \frac{Y_1 + (2G_2 + Y_2 s)s}{2G_2 + (Y_1 + Y_2)s} \tag{7}$$

$$\rho_o = \frac{1 - Y_{in,o}}{1 + Y_{in,o}} = \frac{2G_2(1 - 2G_1) - Y_1{}^2 - Y_1 Y_2 s^2 + [(Y_1 + Y_2)(1 - 2G_1) - 2G_2 Y_1] s}{2G_2(1 + 2G_1) + Y_1{}^2 + Y_1 Y_2 s^2 + [(Y_1 + Y_2)(1 + 2G_1) + 2G_2 Y_1] s} \tag{8}$$

where $s= -j \cot \phi$. To have $\rho_o=0$ at ϕ_3 and ϕ_4, the real and imaginary parts of the numerator must each be zero. Since terms with factors s^2, s^4, s^6, etc. are real and s^1, s^3, s^5, etc.

ductances 1 and 0.5 in the desired bandwidth ϕ_1 to ϕ_2 or f_1 to f_2,[7],[8] (see discussion in Sec. II.) Then ϕ_3 is computed from (13) for the desired band-edge value ϕ_1 or frequency
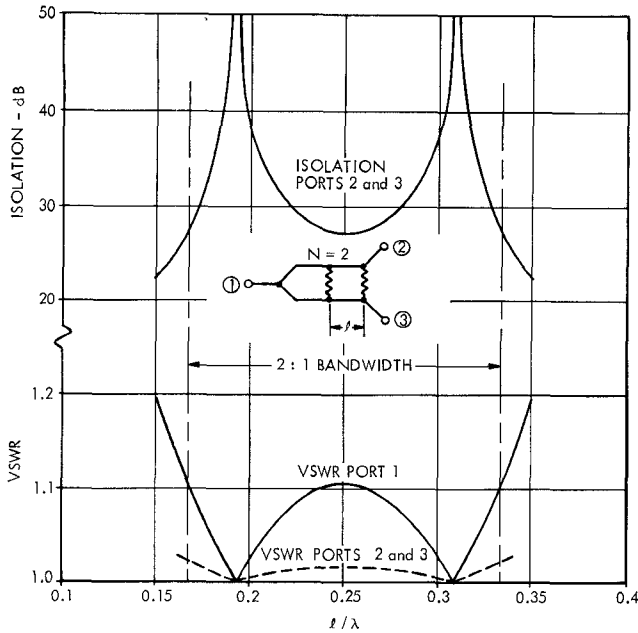
Fig. 5. Response curves for $N=2$, $f_2/f_1=2$ design.

TABLE I
PERFORMANCE LIMITS AND NORMALIZED PARAMETERS OF THREE-PORT
HYBRID DESIGNS

N	2	2	3	3	4	7
f_2/f_1	1.5	2.0	2.0	3.0	4.0	10.0
S_1 (max)	1.036	1.106	1.029	1.105	1.100	1.206
S_2, S_3 (max)	1.007	1.021	1.015	1.038	1.039	1.098
I (min), dB	36.6	27.3	38.7	27.9	26.8	19.4
Z_1	1.1998	1.2197	1.1124	1.1497	1.1157	1.1274
Z_2	1.6670	1.6398	1.4142	1.4142	1.2957	1.2051
Z_3			1.7979	1.7396	1.5435	1.3017
Z_4					1.7926	1.4142
Z_5						1.5364
Z_6						1.6597
Z_7						1.7740
R_1	5.3163	4.8204	10.0000	8.0000	9.6432	8.8496
R_2	1.8643	1.9602	3.7460	4.2292	5.8326	12.3229
R_3			1.9048	2.1436	3.4524	8.9246
R_4					2.0633	6.3980
R_5						4.3516
R_6						2.5924
R_7						4.9652

bandwidth ratio f_2/f_1. Finally (11) and (12) yield R_1 and R_2.[1] Note that Z_1, Z_2, R_1 and R_2 apply to the normalized case, $Z_0=1$. In the general case $Z_0\neq1$ these values should be multiplied by Z_0.

As a design example let $f_2/f_1=2$, corresponding to fractional bandwidth $W=2(f_2/f_1-1)/(f_2/f_1+1)=0.6667$. Young's transformer tables[8] include the desired 2:1 impedance transformation ($R=2$ in his notation), but his nearest W values are 0.6 and 0.8, for which $Z_1=1.21360$ and 1.23388, respectively. Interpolation yields $Z_1=1.2197$ at $W=0.6667$. Then $Z_2=2/Z_1=1.6398$. Equation (13) gives $\phi_3=68.79°$, and (11) and (12) give $R_2=1.9602$ and $R_1=4.8204$. The exact response curves for this case were computed using the analysis method of Section II. The resulting curves plotted in Fig. 5 show that in the desired 2:1 band the maximum VSWR's at ports 1, 2, and 3 are $S_{1m}=1.106$ and $S_{2m}=S_{3m}=1.021$, while minimum isolation between ports 2 and 3 is 27.3 dB. (S_1, S_2, S_3 are the VSWR's at ports 1, 2, 3. The additional subscript m denotes the maximum VSWR in the design bandwidth.) The very slight deviations of $S_2=S_3$ and I_{23} from optimum at the band edges are due to the approximation in (13), and the fact that ρ_e and ρ_o are optimized rather than $S_2=S_3$ and I_{23}. Nevertheless, these deviations are so small as to be safely ignored. The normalized element values and the performance limits are tabulated in Table I.

The case $N=2$ and $f_2/f_1=1.5$ has also been computed, and the results are included in Table I. The highest VSWR is 1.036 and the minimum isolation is 36.6 dB in the 1.5:1 design bandwidth.

A two-section stripline experimental model was constructed for the 1 to 2 GHz band. Maximum VSWR was 1.20

and minimum isolation was 22 dB. The deviation of this measured performance from the theoretical was the result of discontinuity effects which were not compensated in this model.

V. ITERATIVE APPROXIMATION, $N=3$

As shown in Section III, the characteristic impedances Z_1, Z_2, and Z_3 are determined as those values that produce an optimum stepped transformation between resistance levels 1 and 2. Because of the complexity of a synthesis approach for $N=3$, the resistances R_1, R_2, and R_3 have been determined by iterative comuptation leading to approximately optimum performance in the desired bandwidth.

The following facts assist the choice of trial values of $2G_1$, $2G_2$, and $2G_3$ in Fig. 3(d). First, at center frequency the optimum $|\rho_o|$ response function for N odd is zero at $\phi=90°$. Therefore, $Y_{in,o}=1$ when the section lengths are $\lambda/4$, and $2G_1$, $2G_2$, and $2G_3$ must satisfy

$$2G_1 + \cfrac{Y_1^2}{2G_2 + \cfrac{Y_2^2}{2G_3}} = 1.$$

Second, the results for $N=2$ suggest that a good trial value for $2G_N$ is 1.0. Third, the input conductance $2G_1$ should be somewhat smaller than in the $N=2$ case, since the input power is absorbed by three conductances rather than two. A reasonable initial value is two-thirds of the $N=2$ value of $2G_1$, and therefore about 0.26.

The first case treated was $f_2/f_1=3$. The fractional bandwidth is $W=2(3-1)/(3+1)=1$. Young's tables[8] give $Z_1=1.1497$, $Z_2=1.4142$, $Z_3=1.7396$, and also $S_{em}=1.11$. (S_e is the even-mode VSWR. Subscript m denotes maximum or ripple-level VSWR in design band.) Equation (14) and the other two conditions for $2G_1$, $2G_2$, and $2G_3$ were used to determine an initial set of conductance values. The input
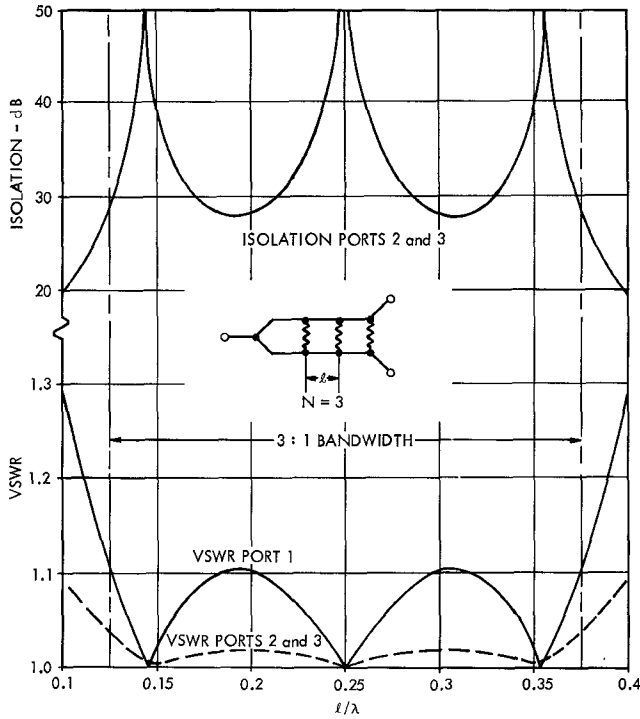
---

[1] If the conductor pairs are not sufficiently decoupled, values of Z_k (even) and Z_k (odd) will differ significantly. In that case Z_k (even) should conform to the stepped transformer design, and Z_k (odd) should be used in (11) and (12).

Fig. 6. Response curves, $N=3$, $f_2/f_1=3$.

VSWR, S_o, of the odd-mode circuit [Fig. 3(d)] was then calculated at points between $\phi=45°$ and $90°$, corresponding to the lower half of the desired 3:1 bandwidth. Because the response is symmetrical, this also determines the upper half. The maximum VSWR was $S_{om}=1.08$. After several judicious changes, the following set of conductances yielded $S_{om}=1.064$ and almost optimum response shape in the desired 3:1 band: $2G_1=0.25$, $2G_2=0.4729$, and $2G_3=0.933$. The computed response curves are plotted in Fig. 6. In the 3:1 design band the minimum isolation is 27.9 dB and the maximum VSWR's are $S_{1m}=1.105$ and $S_{2m}=S_{3m}=1.038$. A

$\rho_{1e}=0.070$	$\rho_{1o}=-0.057$	$T_{1o}=0.772$	ρ_{1o}	$=-0.057$
$\rho_{2e}=0.103$	$\rho_{2o}=-0.152$	$T_{2o}=0.584$	$T_1\rho_{2o}$	$=-0.117$
$\rho_{3e}=0.103$	$\rho_{3o}=-0.362$	$T_{3o}=0.330$	$T_1T_2\rho_{3o}$	$=-0.164$
$\rho_{4e}=0.070$	$\rho_{4o}=-1$		$T_1T_2T_3\rho_{4o}$	$=-0.148.$

A second $N=3$ case for $f_2/f_1=2$ resulted in 38.7 dB minimum isolation and maximum VSWR's $S_{1m}=1.029$ and $S_{2m}=S_{3m}=1.015$. The normalized design parameters and performance limits of the two cases are included in Table I.

VI. GENERAL DESIGN FORMULAS, $N \geq 3$

Because of the difficulties of exact synthesis for $N>2$ and iterative approximation for $N>3$, an approximate approach applicable to all values of N was investigated. The resulting design formulas are simple and have proved to yield good results in several test cases for $N=3$, 4, and 7.

The approximate approach is similar to that used in stepped-transformer analysis.[7] Assume a wave traveling

toward the right in Fig. 3(d). The odd-mode input reflection coefficient may be expressed as the summation of individual reflections from the junction discontinuities. Thus

$$\rho_o = \rho_{1o} + \rho_{2o}t_{1o}^+t_{1o}^-e^{-j2\phi} + \rho_{3o}t_{1o}^+t_{1o}^-t_{2o}^+t_{2o}^-e^{-j4\phi} + \cdots$$

$$+ \rho_{N+1,o}t_{1o}^+t_{1o}^-t_{2o}^+t_{2o}^- \cdots t_{No}^+t_{No}^-e^{-j2N\phi}$$

$$+ \sum_{k=2}^{\infty} b_k e^{-j2k\phi}. \qquad (15)$$

The terms with factors ρ_{10} to $\rho_{N+1,0}$ represent first-order reflections; that is, wave paths with one direction reversal. The summation from $k=2$ to ∞ represents all higher-order reflections; that is, wave paths with three, five, seven, etc., direction reversals at the various reflection points. The formula for ρ_{k0} at the junction of Y_{k-1} and Y_k, with $2G_k$ in shunt, is as follows for a wave incident from the left

$$\rho_{ko} = \frac{Y_{k-1} - Y_k - 2G_k}{Y_{k-1} + Y_k + 2G_k}, \quad k \leq N; \quad \rho_{N+1,o} = -1. \qquad (16)$$

(Note that $Y_{k-1} = Y_0 = 1$ at $k=1$). The product of the transmission coefficients for right- and left-hand travel past junction k is

$$T_{ko} = t_{ko}^+t_{ko}^- = \left(\frac{2Y_{k-1}}{Y_{k-1} + Y_k + 2G_k}\right)\left(\frac{2Y_k}{Y_k + Y_{k-1} + 2G_k}\right)$$

$$= \frac{4Y_{k-1}Y_k}{(Y_{k-1} + Y_k + 2G_k)^2}; \quad k = 1 \text{ to } N. \qquad (17)$$

Equations (15), (16), and (17) also apply to even-mode excitation, except that $G_k=0$, $G_L=0.5$, and $\rho_{N+1,e}=(Y_N-0.5)/(Y_N+0.5)$.
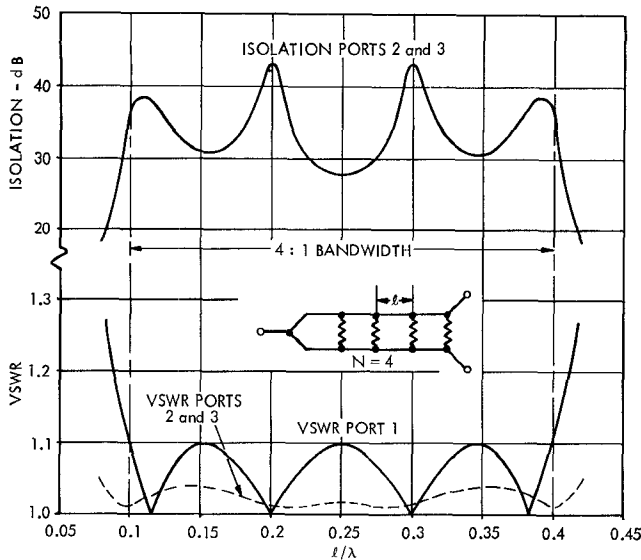
In order to explore this approach, the individual first-order reflection terms were computed for the designs already obtained; that is, $N=2$, $f_2/f_1=1.5$ and 2, and $N=3$, $f_2/f_1=2$ and 3. For example, the case $N=3$, $f_2/f_1=3$ has significant quantities as listed below

In the even-mode case, all ρ_{ke} values are small compared to unity; therefore, only first-order reflection terms need be considered. Also, all T_{ke} values are very near unity and may be replaced by unity in (15). Thus, the following is sufficiently accurate and in fact is the basis of the usual approximate method of stepped-transformer design.

$$\rho_e = \rho_{1e} + \rho_{2e}e^{-j2\phi} + \rho_{3e}e^{-j4\phi} + \rho_{4e}e^{-j6\phi}. \qquad (18)$$

The set of ρ_{ko} values starts at $\rho_{1o} \approx -\rho_{1e}$ and progresses rapidly to $\rho_{4o}=-1$. The higher-order reflection terms $b_k e^{-j2k\phi}$ in (15) are, therefore, too large to be neglected.

The symmetrical set of ρ_{ke} factors in (18) yields Chebyshev $|\rho_e|$ response. The corresponding odd-mode set (ρ_{1o}, $T_1\rho_{2o}$,

Fig. 7. Response curves, $N=4$, $f_2/f_1=4$.

Fig. 8. Response curves, $N=7$, $f_2/f_1=10$.

$T_1T_2\rho_{3o}$, $T_1T_2T_3\rho_{4o}$) is numerically unsymmetrical and cannot yield Chebyshev $|\rho_o|$ response without the aid of the infinite series of higher-order reflection terms contained in (15). To include these higher-order reflections in the approximate analysis would cause enormous complications, and therefore a modified approach was taken.

Careful study of the $N=3$, $f_2/f_1=2$ and 3 cases showed that the following empirical formulas agree well with the conductances obtained by iterative approximation[2]
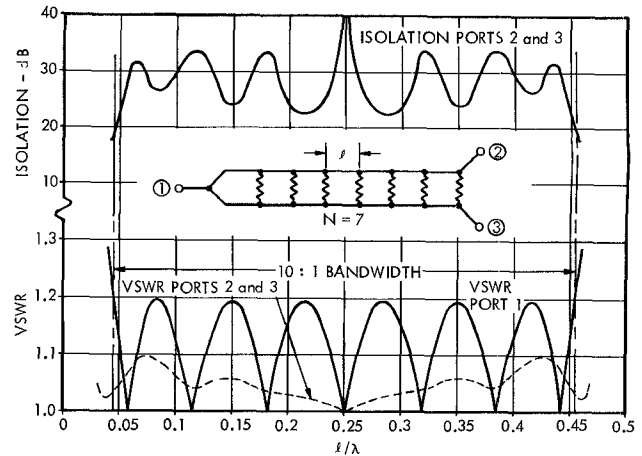
$$G_1 = 1 - Y_1 \tag{19}$$

$$G_k = \frac{Y_{k-1} - Y_k}{Y_{k-1}T_1T_2 \cdots T_{k-1}}, \qquad k = 2 \text{ to } N - 1. \tag{20}$$

After G_1, G_2, $\cdots$, G_{N-1} are computed, G_N is determined such that $Y_{\text{in},o}=1+0.7$ $(S_{e,90^\circ}-1)$ at $\phi=90^\circ$. $S_{e,90^\circ}$ is the even-mode stepped-transformer VSWR at $\phi=90^\circ$. With Chebyshev response, $S_{e,90^\circ}$ equals one for N odd and equals the ripple value S_{em} for N even. G_N is given explicitly by the following finite continued fraction

The maximum VSWR's and minimum isolation are

$$S_{1m} = S_{em} \tag{22}$$

$$S_{2m} = S_{3m} \approx 1 + 0.2(S_{em} - 1) \tag{23}$$

$$I_m \approx 20 \log_{10}\left(\frac{2.35}{S_{em} - 1}\right) \text{dB} \tag{24}$$

where (22) is exact, and (23) and (24) are approximate. Equations (19), (20), and (21) yield conductances within 4 percent of those obtained by iterative approximation in the cases $N=3$, $f_2/f_1=2$ and 3. For the cases $N=2$, $f_2/f_1=1.5$ and 2, disagreement with the exact conductances is larger, but still does not exceed 14 percent. The nature of (19), (20), and (21) is such that good results were anticipated for N higher than 3. Two trial designs have confirmed this.

The first design was $N=4$, $f_2/f_1=4$. Available stepped-transformer tables[8] give the Z_1 to Z_4 values listed in Table I and also give $S_{em}=1.10$. Equations (1), (17), (19), (20), and (21) yield the R_1 to R_4 values listed in Table I. Fig. 7

$$G_N = \cfrac{\tfrac{1}{2}Y_{N-1}^2}{-2G_{N-1} + \cfrac{Y_{N-2}^2}{-2G_{N-2} + \cfrac{Y_{N-3}^2}{\begin{array}{c}\cdot\\\cdot\\\cdot\end{array}}}} \qquad\qquad \begin{aligned} S_{e,90^\circ} &= 1, \quad N \text{ odd} \\ &= S_{em}, \quad N \text{ even}\end{aligned}$$

$$\cfrac{}{-2G_2 + \cfrac{Y_1^2}{-2G_1 + 1 + 0.7(S_{e,90^\circ} - 1)}} \cdot \tag*{[(21)]}$$

[2] The heuristic reasoning leading to (19), (20), and (21) and suggesting their applicability for $N>3$ is rather lengthy and cannot be supported rigorously. These formulas are justified, however, by the computed results presented in this paper. The factor 0.7 in (21) was chosen for best empirical fit.

shows the response curves calculated for this case by the meteod of Section II. The excellent isolation and VSWR performance suppor tthe utility of the approximate design formula.

The second design was $N=7$, $f_2/f_1=10$. Stepped-transformer formulas[7] are used in this case, since tables are not available for $N>4$.[3] These formulas yield the Z_1 to Z_7 values in Table I. Another formula[7] gives $\rho_{em}=0.0882$ as the reflection-coefficient ripple level. The corresponding VSWR is $S_{em}=(1+\rho_{em})/(1-\rho_{em})=1.191$. Equations (1), (17), (19), (20), and (21) result in the R_1 to R_7 values in Table I. The computed response curves are plotted in Fig. 8. Over the 10:1 design bandwidth $I_m=19.6$ dB, $S_{1m}=1.206$, and $S_{2m}=S_{3m}$ $=1.100$. This performance is good but not optimum. In a 9:1 band, $I_m=22.0$ dB, $S_{1m}=1.197$, and $S_2=S_3=1.100$.

Equation (24) yields minimum isolation values within 1.0 dB of the computed isolation curves in all examples for $N=2$, 3, and 4. For $N=7$ and $f_2/f_1=10$, (24) is accurate inside the band, but at the band edges the computed isolation curve is lower by 3 dB. Equation (23) for S_{2m} and S_{3m} is fairly good near band center but not toward the band edges. However, in none of the examples do S_{2m} and S_{3m} exceed $1+0.5(S_{em}-1)$. These rather small discrepancies in values from (23) and (24) are apparently mainly the result of the nonoptimum design examples rather than failures of the equations themselves.

VII. CONCLUSIONS

The hybrid power divider's bandwidth increases with its number of sections. The upper limit of generally useful bandwidth versus the number of sections is about as follows: 2.5:1 for two sections; 4:1 for three sections; 5.5:1 for four sections; and 10:1 for seven sections

The two-section hybrid power divider has sufficient bandwidth for most applications. Its design by means of the exact formulas in Section IV is straightforward and rapid.

---

[3] Tables published by Levy[9] extend to $N=21$. In his notation $L=0.512$ dB corresponds to the desired 2 to 1 impedance transformation. The range of Levy's tables excludes this value of L for $N \geq 5$ and $S_{em}>1.02$. With $S_{em}=1.02$ instead of a generally acceptable 1.10 or 1.20 value, bandwidths are unduly restricted.

The approximate formulas in Section VI have yielded designs with good performance in the cases tested; namely, $N=3$, $f_2/f_1=2$ and 3; $N=4$, $f_2/f_1=4$; $N=7$, $f_2/f_1=10$. Similar results for other values of N and f_2/f_1 may be reasonably expected. However, until additional examples are tested, a safe practice would be to verify each design by computing its VSWR and isolation response by the method of Section II. If these curves deviate excessively from optimum, the R_k values may then be refined by iterative approximation; that is, by judiciously altering the R_k values and recomputing the response curves until the performance is considered sufficiently near optimum.

REFERENCES

[1] E. J. Wilkinson, "An N-way hybrid power divider," *IRE Trans. Microwave Theory and Techniques*, vol. MTT-8, pp. 116–118, January 1960.

[2] J. R. Dent, "Strip-line technique produces a simple 3-dB directional coupler," *Electronic Design*, pp. 52–53, August 31, 1960.

[3] L. I. Parad and R. L. Moynihan, "Split-tee power divider," *IEEE Trans. Microwave Theory and Techniques*, vol. MTT-13, pp. 91–95, January 1965.

[4] S. David, "A wideband coaxial-line power divider," *IEEE Trans. Microwave Theory and Techniques (Correspondence)*, vol. MTT-15, pp. 270–271, April 1967.

[5] J. Reed and G. J. Wheeler, "A method of analysis of symmetrical four-port networks," *IRE Trans. Microwave Theory and Techniques*, vol. MTT-4, pp. 246–252, October 1956.

[6] P. I. Richards, "Resistor-transmission-line circuits," *Proc. IRE*, vol. 36, pp. 217–220, February 1948.

[7] S. B. Cohn, "Optimum design of stepped transmission-line transformers," *IRE Trans. Microwave Theory and Techniques*, vol. MTT-3, pp. 16–21, April 1955. This reference gives formulas applicable to all values of N.

[8] L. Young, "Tables for cascaded homogeneous quarter-wave transformers," *IRE Trans. Microwave Theory and Techniques*, vol. MTT-7, pp. 233–238, April 1959. (This reference provides design tables for $N=2$, 3, and 4). Also see "Correction," *IRE Trans. Microwave Theory and Techniques*, MTT-8, pp. 243–244, March 1960. (The "Correction" applies to $N=4$).

[9] R. Levy, "Tables of element values for the distributed low-pass prototype filter," *IEEE Trans. Microwave Theory and Techniques*, vol. MTT-13, pp. 514–536, September 1965.